GEOPHYSICS, VOL. 73, NO. 2 (MARCH-APRIL 2008); P. V11–V18, 5 FIGS.
10.1190/1.2831936

Time-varying wavelet estimation and deconvolution by kurtosis maximization

Mirko van der Baan[1]

ABSTRACT

Phase mismatches sometimes occur between final processed sections and zero-phase synthetics based on well logs, despite best efforts for controlled-phase acquisition and processing. The latter are often based on deterministic corrections derived from field measurements and physical laws. A statistical analysis of the data can reveal whether a time-varying nonzero phase is present. This assumes that the data should be white with respect to all statistical orders after proper deterministic corrections have been applied. Kurtosis maximization by constant phase rotation is a statistical method that can reveal the phase of a seismic wavelet. It is robust enough to detect time-varying phase changes. Phase-only corrections can then be applied by means of a time-varying phase rotation. Alternatively, amplitude and phase deconvolution can be achieved using time-varying Wiener filtering. Time-varying wavelet extraction and deconvolution can also be used as a data-driven alternative to amplitude-only inverse-Q deconvolution.

INTRODUCTION

Controlled-phase acquisition and processing plays an important role in current acquisition and processing strategies (Trantham, 1994). Deterministic corrections such as for debubbling and for attenuation-related dispersion are favored over statistical approaches. Nevertheless, despite the best efforts to control the phase of a wavelet during the entire acquisition and processing sequence, phase mismatches regularly occur between final processed data based on deterministic zero-phase shaping and zero-phase synthetics created from well logs. The existing well logs are often used in these cases as ground truth, and a further phase correction is applied to the data such that they match the zero-phase synthetics.

Unfortunately, well logs are not always available, and different wells can predict different phase corrections. It is also possible that the phase mismatch varies with time. Thus, there is a need for a statistical approach to estimate the phase of a wavelet from the data alone, yielding complementary information, and to serve as additional quality control.

Levy and Oldenburg (1987), Longbottom et al. (1988), and White (1988) describe such a technique for stationary data. Their method is based on a simplification of the blind deconvolution method proposed by Wiggins (1978). They search for a constant-phase rotation (i.e., a frequency-independent one) that renders the data maximally non-Gaussian. The rationale behind the Wiggins algorithm and variants is that convolution of any filter with a time series that is white with respect to all statistical orders renders the outcome more Gaussian. The optimum deconvolution filter is therefore one that ensures the deconvolution output is maximally non-Gaussian (Donoho, 1981). The constant-phase assumption made by Levy and Oldenburg (1987), Longbottom et al. (1988), and White (1988) greatly reduces the number of free parameters and thus stabilizes the performance of their algorithm compared with the Wiggins method. Wavelets derived in seismic-to-well ties often have a near-constant phase, thus justifying this assumption (Longbottom et al., 1988).

I extend the constant-phase rotation method in three ways. First, I modify it such that it can handle nonstationary (i.e., time-varying) data. Second, I show how the time-varying wavelet can be extracted, which can serve as a more familiar quality-control tool for interpreters than phase information alone. Finally, I demonstrate how time-varying amplitude and phase deconvolution can be applied by means of Wiener filtering. The latter has an optimum trade-off between noise amplification and recovery of the reflectivity series (Berkhout, 1977). I illustrate the method on both synthetic and real data examples and discuss some quality-control measures to determine whether the extracted phase variations are reliable.

METHOD

Phase estimation

To estimate the phase of the wavelet, I use a simplification of the blind deconvolution method developed by Wiggins (1978). The ob-

Manuscript received by the Editor 27 June 2007; revised manuscript received 6 September 2007; published online 12 February 2008.
[1]University of Leeds, School of Earth and Environment, Leeds, U.K. E-mail: m.van-der-baan@see.leeds.ac.uk.

jective of blind deconvolution is to retrieve the reflectivity series without knowing the amplitude or phase spectrum of the wavelet. Blind deconvolution therefore differs from conventional deconvolution in that we do not make a priori assumptions about the wavelet phase as is routinely done in, for example, predictive deconvolution (gapped/spiking) or spectral whitening.

Wiggins (1978) introduced the first blind deconvolution algorithm based on kurtosis maximization. Convolving any white reflectivity series with an arbitrary wavelet renders the outcome less white but also more Gaussian (Donoho, 1981). Maximizing the kurtosis recovers the original reflectivity series because kurtosis measures deviation from Gaussianity. The technique can handle nonminimum-phase wavelets because kurtosis is a fourth-order statistic and higher-order statistics retain phase information — contrary to conventional algorithms based on second-order statistics, such as predictive deconvolution and spectral whitening.

The Wiggins algorithm and variants attracted significant attention until the mid-1980s, when the method was found to have several shortcomings. It tends to emphasize the largest reflector at the expense of all others, and it is unstable for very band-limited data (Wiggins, 1985; Longbottom et al., 1988; White, 1988). In particular, if the principal frequency is larger than the wavelet passband (i.e., roughly less than 1.5 octaves of bandwidth), then the Wiggins algorithm breaks down.

Levy and Oldenburg (1987), Longbottom et al. (1988), and White (1988) greatly reduced the number of degrees of freedom in the phase-estimation problem by proposing that a seismic wavelet in the later processing stages can be described accurately by a constant-phase approximation, leaving only a single degree of freedom and thereby a robust inversion procedure. The optimum phase is estimated by applying a series of constant-phase rotations to the data. The angle corresponding to the maximum kurtosis value determines the most likely wavelet phase.

The normalized kurtosis of a discrete time series $x(t)$ is commonly approximated by

$$\text{kurt}(x) = n\frac{\sum x^4(t)}{\left[\sum x^2(t)\right]^2} - 3, \tag{1}$$

with n the number of time samples and t discrete time.

The constant-phase rotations can be applied naturally in the frequency domain. Arons and Yennie (1950) show, however, that a time-domain implementation is also possible and much faster. The rotated trace x_{rot} can be computed from the original trace x by

$$x_{\text{rot}}(t) = \cos\phi x(t) + \sin\phi H[x(t)], \tag{2}$$

with ϕ the phase rotation angle and $H[.]$ the Hilbert transform. A further advantage of time-domain implementation is that it is straightforward to apply time-varying rotations because each individual time sample is treated independently.

The most likely phase angle ϕ_{kurt} corresponds to the maximum kurtosis value. This is easiest estimated using a grid search with test angles ϕ between $-180°$ and $180°$. The kurtosis is averaged over tens of traces to ensure robustness.

The kurtosis variation with test angle ϕ can be used as a quality-control tool. It should display a dominant $\cos 2\phi$ variation, with possibly a $\cos 4\phi$ trend superposed (White, 1988). The difference between the maximum and minimum kurtosis value indicates the robustness of the inversion result (Levy and Oldenburg, 1987; Longbottom et al., 1988; White, 1988).

Because of the large reduction in degrees of freedom, the described phase-estimation method by kurtosis maximization can be extended to cope with time-varying phase changes by subdividing each section into partly overlapping time windows. A single phase is estimated for each window. An overlap of 67% is used such that rapid phase changes indicate the window size is likely to be too small. The extracted phase is assigned to the center of each analysis window. A linear interpolation, done between each center position, recovers the phase variations in between evaluation points. At the start and end times, the wavelet phase is assumed to be constant.

The chosen implementation assumes that the phase change of the wavelet is smooth enough to be treated as piecewise stationary within each window. The interpolation between evaluation windows softens this assumption thereafter. It also assumes that the phase spectrum of the reflectivity as a function of frequency is a uniformly distributed random process with all angles equally likely.

If phase-only deconvolution is desired, it can be accomplished by expression 2 as well. In this case, the rotation angle ϕ becomes time dependent and is exactly equal to minus the time-varying phase just extracted from the kurtosis analysis, or $-\phi_{\text{kurt}}(t)$.

Wavelet estimation

Wavelet estimation is straightforward once the phase is known. Only the amplitude spectrum is left to be estimated. This is done by (1) averaging the amplitude spectra of all traces in each time window and (2) multiplying the averaged window in the time domain by a Hanning taper for enhanced robustness, while (3) ensuring that the amplitude at the Nyquist frequency remains zero. This procedure leads to a symmetric, zero-phase wavelet. It naturally assumes that the reflectivity within each analysis window is a white process. The multiplication in the time domain with a Hanning filter serves two purposes: It smoothes the spectral estimate, thus ensuring extra robustness, and it allows for the inclusion of any a priori information on the expected wavelet lengths.

Inspection of the time-domain wavelet and its variations with time is another useful quality control. In the frequency domain, each individual wavelet W_j is given by

$$W_j(f) = |W_{\text{ave},j}(f)|\exp\{i\phi_{\text{kurt},j}\,\text{sgn}(f)\}, \tag{3}$$

with $|W_{\text{ave},j}|$ the averaged amplitude spectrum, $\phi_{\text{kurt},j}$ the constant-phase angle determined by evaluating the kurtosis in window j, and sgn(.) the sign function.

Time-varying Wiener filtering

In the deconvolution problem, we assume that the observed trace x is the result of the convolution of the wavelet w with the reflectivity series r plus some superposed noise n. That is,

$$x(t) = w(t) * r(t) + n(t), \tag{4}$$

where $*$ indicates convolution and t represents time. The objective is to find a filter $g(t)$ such that the outcome $y(t)$ is as close as possible to the original reflectivity series $r(t)$. Thus, $y(t) = g(t) * x(t) \approx r(t)$. Because of the presence of the noise, the reflectivity series r cannot be recovered perfectly and a compromise must be achieved between noise amplification and successful recovery.

If the wavelet $w(t)$ is known, then the time-domain Wiener filter $g_w(t)$ achieves an optimum solution. In the frequency domain, it is given by

$$G_w(f) = \frac{W^*(f)}{|W(f)|^2 + \sigma_n^2}, \quad (5)$$

with f the frequency, σ_n^2 the noise variance, and superscript $*$ the complex conjugate (Berkhout, 1977).

Time-varying deconvolution is conceptionally slightly more complex than the ordinary stationary case because the filter coefficients change with time. Formally, it is written as (Clarke, 1968; Wang, 1969)

$$y(t) = \int_{-\infty}^{\infty} g_w(t - t', t')x(t')dt', \quad (6)$$

with t and t' the observation and initiation times, respectively. The time difference $\tau = t - t'$ serves a similar purpose to the normal lag τ in stationary convolution, but the outcome $y(t)$ observed at t depends on the initiation time t' of both the input trace x and the filter g_w. The latter also varies with lag τ from the initiation time t'.

Equation 6 represents a time-domain implementation. However, I choose a frequency-domain implementation that is conceptually simpler and easier to implement at the expense of a slight increase in computation time.

A specific Wiener filter is created for each individual wavelet $W_j(f)$ estimated in window j using expressions 3 and 5. The estimated wavelets and all traces are zero padded such that they have the same length; this ensures that wraparound effects resulting from circular convolution in the frequency domain are prevented. Each individual Wiener filter thus created is applied to all traces in their entirety. Linear interpolation of the resulting deconvolved sections $y_j(t)$ then yields the final deconvolved section $y(t)$. Expressed by

$$y(t) = [1 - r(t)]y_j(t) + r(t)y_{j+1}(t), \quad (7)$$

with

$$r(t) = \frac{t - t_j}{t_{j+1} - t_j}, \quad \forall t \in [t_j, t_{j+1}[, \quad (8)$$

where y is the final deconvolved trace and y_j is the deconvolved trace obtained using the jth wavelet estimated with an analysis window centered at position t_j. At the start and end times, it is assumed that the deconvolution result $y(t)$ equals the Wiener output of the first and last wavelet exactly.

Implementation

The technique can be implemented in the described order, i.e., phase estimation by kurtosis maximization, wavelet estimation by spectral averaging, and then time-varying Wiener filtering. This has the advantage that one can stop after the first step if time-varying phase-only deconvolution is desired.

Alternatively, one can estimate a zero-phase wavelet first in each analysis window, deconvolve it by means of Wiener filtering, and estimate the phase using kurtosis maximization on the outcome. The advantage of this approach is that it leads to a more accurate phase estimate. The Wiener filtering reduces the influence of the noise while boosting the kurtosis value, thus increasing the contrast between the minimum and maximum values found. One can then proceed with phase-only or amplitude-and-phase deconvolution as described before.

In both cases, care should be taken when combining the deconvolution outcomes for the different wavelets. The lowest reconstruction error is obtained if the Wiener filter (equation 5) for each wavelet $W_j(f)$ is applied on the entire trace length in the case of a frequency-domain implementation. Least-squares filter design is needed if a time-domain implementation is desired (Berkhout, 1977).

RESULTS

Synthetic example

To illustrate the entire procedure, I use a challenging synthetic example composed of a super-Gaussian reflectivity convolved with two superposed Ricker wavelets with time-varying peak frequencies and phases. At zero time, the composite wavelet has peak frequencies and phases of, respectively, (30 Hz, $-90°$) and (60 Hz, $-30°$), which linearly transform to (15 Hz, 30°) and (30 Hz, 90°) at the bottom of the recording. The peak frequencies are thus halved from top to bottom, and the wavelet phase is at every instant frequency dependent (Figure 1a). The total recording time is 2 s, with a sample rate of 2 ms. There are 30 traces.

The reflectivity series is created by raising a white Gaussian time series to the third power. This results in a super-Gaussian reflectivity series with both isolated and closely spaced events but without hard zeros. Random Gaussian noise is superposed on each trace after convolution of the reflectivity series with the composite wavelet such that the signal-to-noise ratio (S/N) is three. That is, the standard deviation of the signal is three times that of the noise.

Figure 2a displays the original data. The reduction of frequency content with time, is clearly visible. Figure 1a shows the true wavelet at various times. Its peak frequency and phase vary considerably with time, rendering this a challenging test.

I use nine 0.56-s windows with a 67% overlap in the wavelet estimation procedure. The extracted wavelets are 60 ms long. Figure 1b shows the extracted wavelets, and Figure 1c shows the estimated wavelet phase interpolated to all recording times. It also shows the average phase of the composite wavelet for guidance. The extracted and instantaneous wavelets compare very well, as do the estimated and averaged phases. In general, phase mismatches up to 20° produce only minor changes in associated waveforms — something also noticed by Levy and Oldenburg (1987).

This example is challenging for several reasons. The phases changes are dramatic and frequency dependent, yet the constant-phase approximation holds well. The frequency content of the composite wavelet also varies considerably. Tests show that the constant-phase approximation works well even if a third Ricker wavelet is added with yet another phase. Only the introduction of time lags between the different wavelets (thus mimicking significant dispersion) or phase variations of more than 90° seem to pose problems.

The kurtosis variations with test angle ϕ for the first, middle, and last wavelet are shown in Figure 1d. The other phases display similar variations. All curves display variations of 100% or more. They are therefore very well resolved. This also holds true for the middle wavelet, which has the largest error in its estimated phase angle. Analysis of the relevant section of the reflectivity series reveals that it is atypical, in that its phase spectrum has a constant bias affecting the wavelet-phase estimate.

The result of phase-only and amplitude-and-phase deconvolution is displayed in Figure 2b and c. Phase-only deconvolution solely applies a phase rotation to the recorded traces using expression 2; it does not change the frequency content. A constant-phase rotation on a monofrequency signal amounts to a simple time shift of the entire trace. Applying a time-varying phase rotation on a seismic signal often results in a gentle squeezing or stretching of the time series. Phase mismatches on continuous sequences of events thus might give the impression that a timing error is occurring. Only if an isolated event can be detected does it become possible to see if the phase rotation was done properly because a zero-phase wavelet is symmetric.

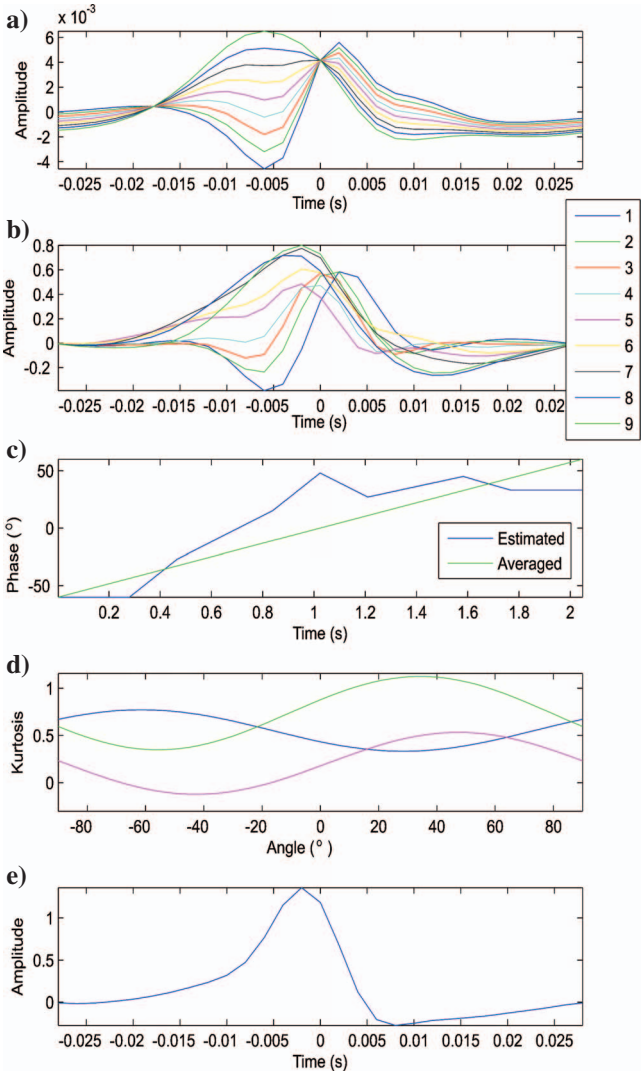

Figure 1. Wavelet estimation results for the synthetic example. (a) Instantaneous wavelets, mixed phase. The true wavelet has a strong time-varying nature, as seen by its instantaneous waveforms shown at nine different times between 0.3 and 1.8 s. (b) Extracted time-varying wavelets, mixed phase. Extracted waveforms are at the same time positions, numbered 1–9 with increasing time. Extracted and instantaneous wavelets bear a good resemblance. (c) Estimated and averaged true phase as a function of time. (d) The kurtosis variations with test angle indicate that each phase is well resolved. (e) Global wavelet, constant phase. Extracting a single constant phase wavelet from the entire section in Figure 2 leads to biased results because the observations are nonstationary. A local kurtosis analysis is needed to cope with the time-varying recordings.

The differences between Figure 2a and b are therefore mostly the result of small changes in arrival time of events. This is best visible in Figure 3, showing the actual reflectivity series, the noisy input data, and various deconvolution outcomes for the first trace. A comparison of Figure 3b and c reveals that mostly subtle differences are visible between the input data and the phase-rotated trace. The exception is the reflection at 0.2 s, which has become zero phase and symmetric after phase rotation.

Time-varying Wiener filtering (expressions 5 and 6, determined using the estimated wavelets of expression 3) corrects for phase and increases the frequency content of the outcome. It whitens the frequency content of traces within the passband of the wavelet (i.e., $|W(f)/\sigma_n^2| \gg 1$) and dampens any noise outside of this frequency range (i.e., $|W(f)/\sigma_n^2| \ll 1$) (Berkhout, 1977). The composite wavelets are already relatively white within their passbands. The result of time-varying amplitude and phase deconvolution (Figure 2c) therefore displays a similar response as for phase-only deconvolution (Figure 2b) but with less noise contamination. This can also be seen in Figure 3b-d.

Finally, estimating a single wavelet for the entire section produces strongly biased results. The extracted global wavelet is shown in Figure 1e, and the associated deconvolution result is shown in Figure 2d. Not only is the global wavelet dissimilar to any of the instantaneous ones (Figure 1a), but also it cannot correct the phase of the data (e.g., reflection at 0.20 s). It is evident that any deconvolution attempt with this wavelet leads to nonoptimal results. Time-varying wavelet estimation and deconvolution must be performed to handle observations of this kind.

Stacked section

In the second example, a stacked section is considered. Figures 4 and 5 display the data before and after deconvolution, the extracted wavelets, and associated phase and kurtosis variations. Five 2.1-s analysis windows are used, each with a 67% overlap. In each window, a 0.1-s-long wavelet is extracted. Predictive deconvolution had already been applied to the data such that only phase corrections were used in the deconvolution.

Phase variations show a steplike change from $-75°$ to $-21°$ (Figure 5c). The kurtosis variations indicate again that the phase is well resolved except possibly for the last wavelet. Relative variations are from 6.5% for the first wavelet to 16% for the deepest four wavelets. A relative fluctuation of 6.5% is low, but the high kurtosis value of four boosts confidence that the angle has been estimated correctly. The last wavelet, on the other hand, has only a kurtosis value of 0.4, indicating the deepest portion of the seismic section is too close to Gaussian to allow for robust phase estimation (Figure 5d). The wavelets broaden with time, indicating the presence of seismic attenuation.

The original data and the result of phase-only deconvolution are shown in Figure 4. Most variations occur in the shallowest part, as seen in Figure 4c and d, which zooms in on the top leftmost corner. Examples where the phase rotation has rendered the reflectors approximately zero phase can be seen at 0.48 and 0.75 s, indicated by the arrows.

Designing a single deconvolution filter does not produce suitable results for this data set. For instance, the global wavelet has a phase

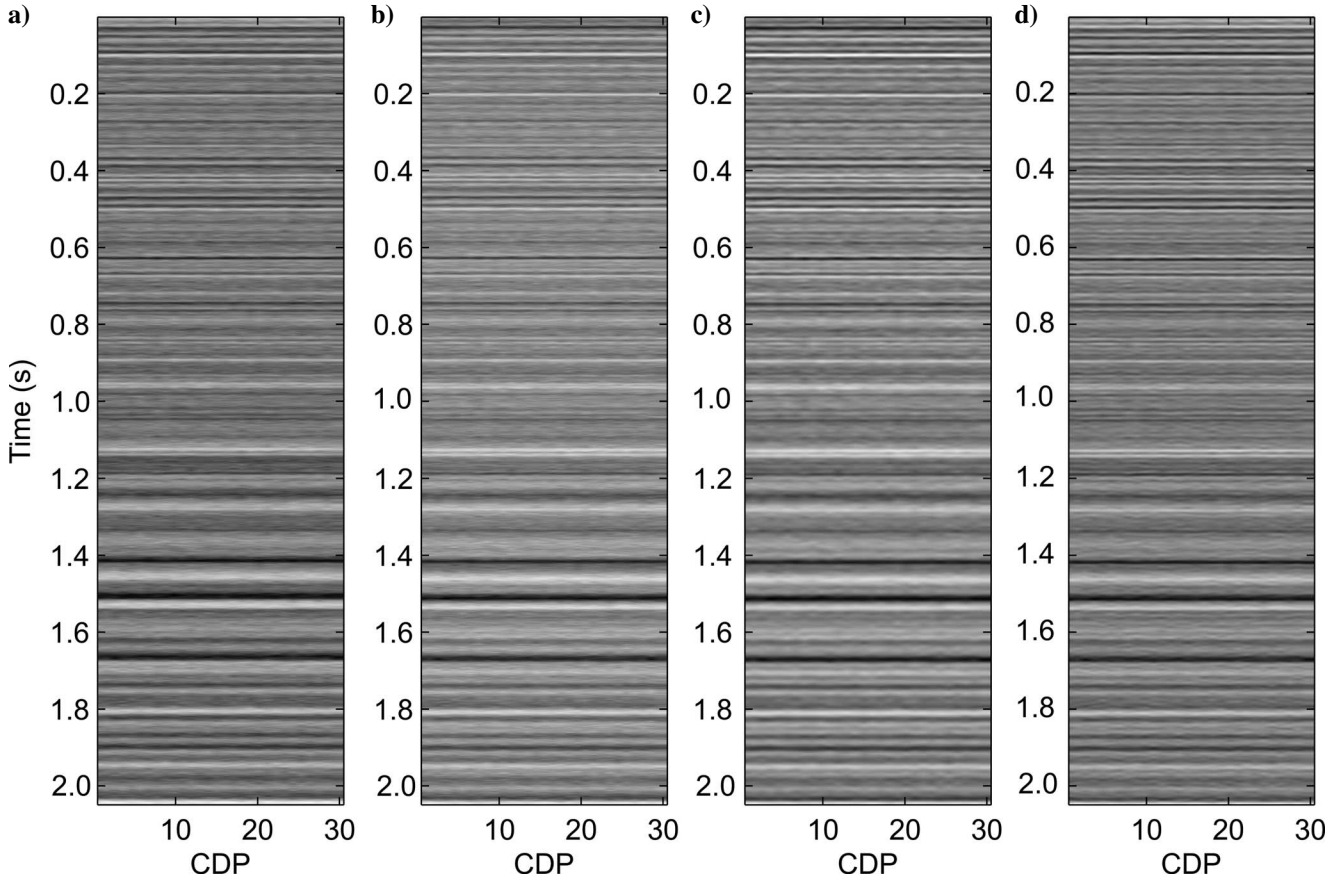

Figure 2. Deconvolution results for the synthetic example. (a) Original input data displaying a strong decrease in the peak frequency with time. Results after (b) time-varying phase-only deconvolution using the estimated phase angle shown in Figure 1c, (c) time-varying amplitude and phase deconvolution using the extracted wavelets (Figure 1b), and (d) global deconvolution using the constant wavelet (Figure 1e). Differences in all deconvolution results are subtle at this scale. They are much clearer if examined on a single trace (Figure 3). CDP = common-depth point.

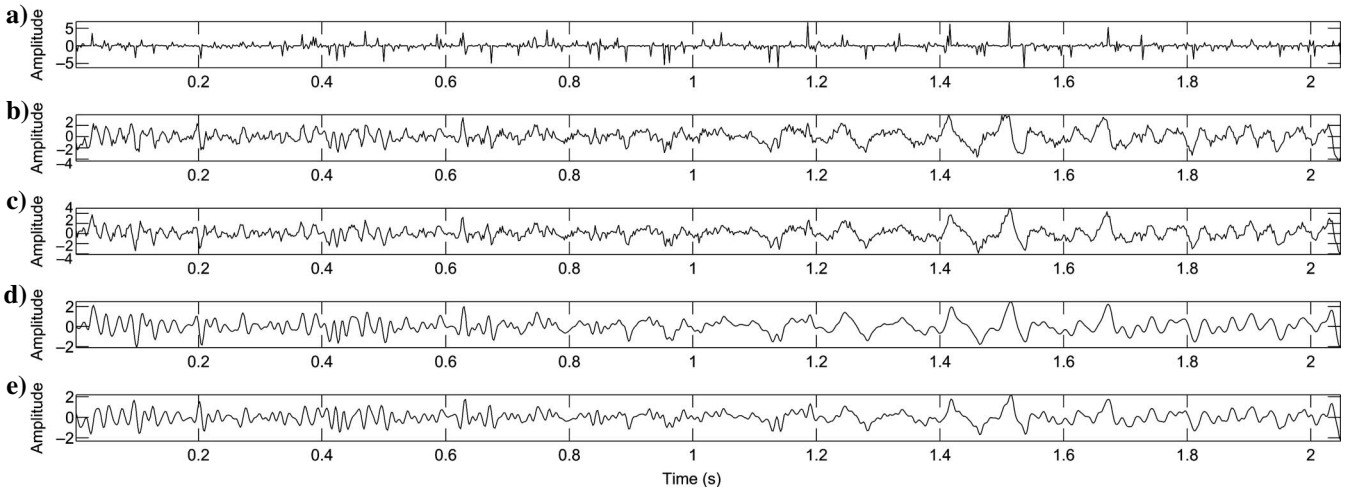

Figure 3. Deconvolution results for the first trace of the synthetic example. (a) Reflectivity series, (b) input data with added noise, (c) results after time-varying phase rotation, (d) results after time-varying amplitude and phase deconvolution, and (e) results after global deconvolution using a constant wavelet. Both time-varying and global deconvolution have removed some of the high-frequency noise outside the passband of the wavelet. However, the global result does not create a zero-phase section because the observations are nonstationary (e.g., reflection at 0.2 s).

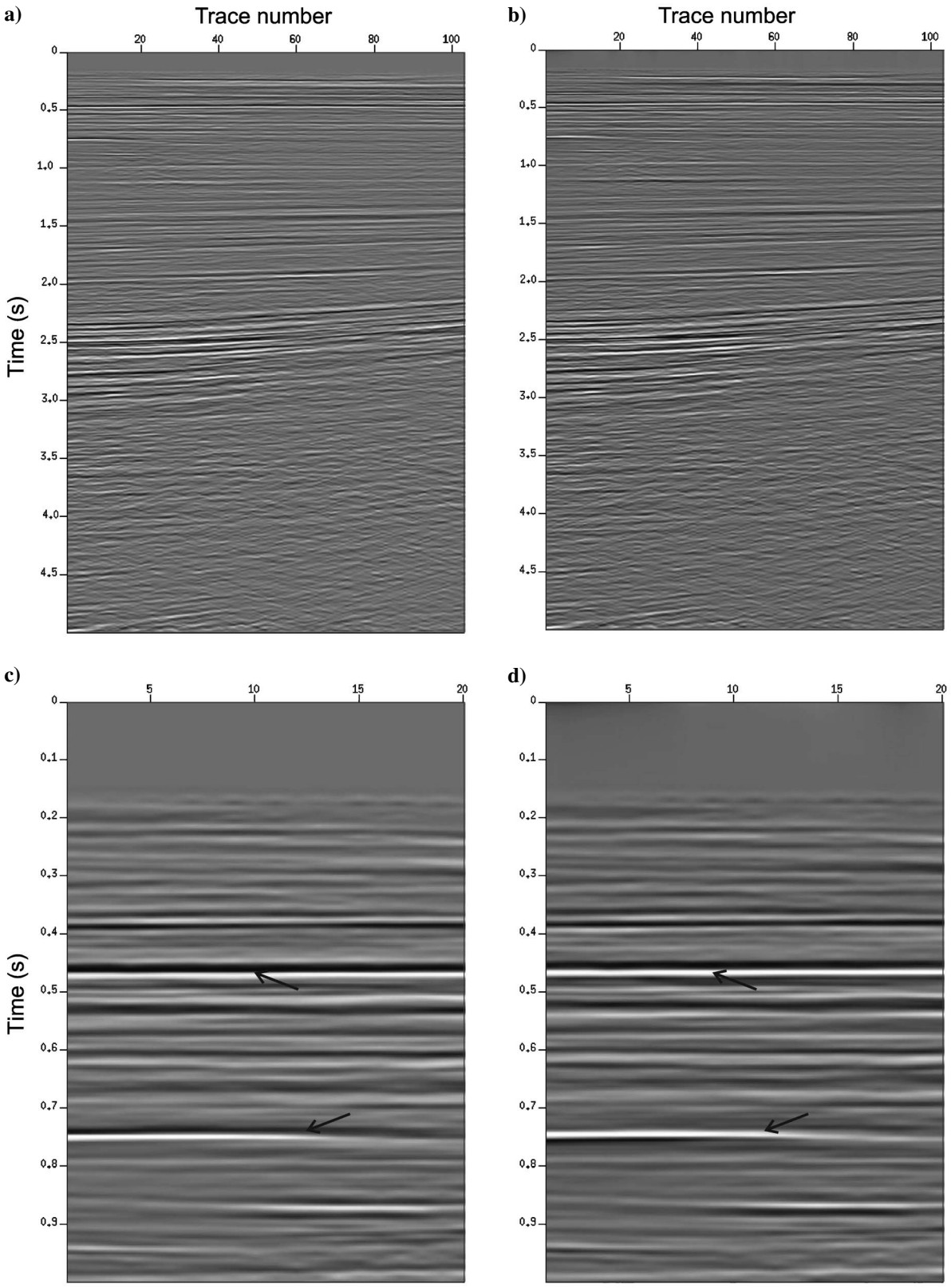

Figure 4. Deconvolution results for stacked section. (a) Original data; (b) outcome after time-varying rotation. (c and d) Close-up of the top-left corner of, respectively, the original and deconvolution result. Several phase rotations are visible, indicated by the arrows. Data courtesy of Shell.

of $-57°$ and contrasts increasingly from the five extracted local wavelets (Figure 5a). Time-varying wavelet extraction and deconvolution are required for this data set.

DISCUSSION

Several assumptions underlie the described wavelet estimation technique. It assumes that the earth's reflectivity series have a white non-Gaussian distribution, i.e., its amplitude spectrum is flat and the phase spectrum has a uniform distribution between $-\pi$ and π radians.

Analysis of well logs has shown that reflectivity series are generally non-Gaussian (Walden and Hosken, 1986) and that they tend to be blue instead of white, thus lacking low vertical wavenumbers (Walden and Hosken, 1985). This nonwhiteness is generally considered to be a second-order problem. It can be remedied easily if local well logs exist (Saggaf and Robinson, 2000).

It is also conceivable that the earth's phase spectrum has a nonuniform distribution at specific depths and locations. Local well-log analyses can again reveal whether this is the case. A local nonuniform phase distribution would bias the estimated wavelet as it happened, for instance, in the fifth wavelet in Figure 1.

The technique further assumes the wavelet varies only smoothly with time, such that it can be treated as piecewise stationary within each analysis window. The linear interpolation between evaluation points softens this assumption to a certain extent. A trade-off exists, however, between the optimum length of the analysis window and the nonstationarity of the wavelet. On the one hand, one needs a sufficiently long window to estimate the kurtosis robustly. On the other hand, the wavelet and its phase should vary only moderately within the analysis window. Robust estimation of the kurtosis is difficult for weakly non-Gaussian and/or short time series (Sacchi and Ulrych, 2000). Analysis windows should contain at least several hundred samples. The use of overlapping windows helps with quality control because rapid variations of estimated wavelets and phases will indicate suspicious results.

Finally, the method assumes that the wavelet has a relatively constant-phase spectrum and that its bandwidth is larger than the peak frequency. Wavelets derived in seismic-to-well ties often have a near-constant phase (Longbottom et al., 1988), thus justifying the first assumption. The constant-phase assumption greatly reduces the number of free parameters and stabilizes the performance of the algorithm. Longbottom et al. (1988) and White (1988) show, nonetheless, that phase estimation by kurtosis maximization is unstable if the peak frequency is larger than the wavelet passband (i.e., less than approximately 1.5 octaves of bandwidth). However, with the advent of the microelectrical-mechanical system sensors, bandwidth is much less of a problem than it was 20 years ago and unlikely to pose a problem in practice.

The cause for the phase variations over time is unknown in the real data example. However, the kurtosis variations with test angle show that the extracted phase is sufficiently well resolved to be determined. Unfortunately, the measured variations could not be confirmed by means of a seismic-to-well tie analysis. It is thus possible that they reflect true geologic changes with depth. A statistical analysis of the measured data alone cannot reveal this. This was not the objective of the article. A statistical approach yields relevant information about the data, which can be used to zero phase time-varying observations, as quality control to check deterministic phase corrections, or even as an individual analysis tool.

The described method can also be used as an alternative to deterministic inverse-Q deconvolution approaches (Robinson, 1979; Bickel and Natarajan, 1985; Hargreaves and Calvert, 1991; Y. Wang, 2002). The latter apply frequency-dependent, phase-only or phase-and-amplitude corrections to the data, given some measured values for the quality factor Q. Unfortunately, inverse-Q amplitude filtering is inherently unstable and may decrease the S/N with increasing time.

The described statistical approach whitens the data only within the passband of the locally extracted wavelet. The damping factor σ_n in expression 5 determines the trade-off between recovery of the reflectivity series and noise amplification. Wiener filtering leads to an optimal trade-off between these two objectives and has the advantage that no Q factor need be measured first. Indeed, it is even possible to estimate the Q factor from the extracted wavelets, e.g., by means of computing spectral ratios or by tracking the shift in their peak frequency (Hauge, 1981; Tonn, 1991; Quan and Harris, 1997).

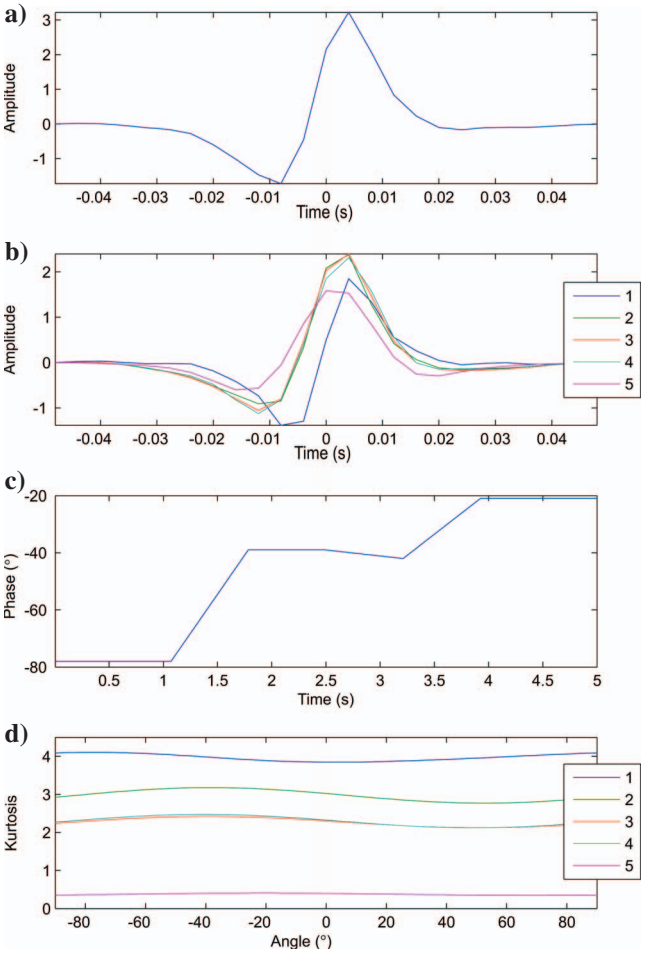

Figure 5. (a) Global wavelet constant phase, (b) time-varying extracted wavelets (constant phase), (c) time-varying phase, and (d) kurtosis variations associated with the real data example in Figure 4. Five wavelets have been extracted, numbered 1–5 with increasing time. Only the middle wavelets are similar to the global wavelet. Wavelets seem to broaden with time, indicating the presence of seismic attenuation. Kurtosis variations for each wavelet suggest that all wavelets are well resolved except for the last one, which has only a small kurtosis value.

Deterministic dispersion corrections, on the other hand, allow for frequency-dependent phase modifications, whereas a single-phase rotation is applied by the statistical method described above.

The noise variance σ_n^2 in the Wiener filter (expression 5) was kept constant in all examples, although it can naturally be varied such that problems caused by nonstationary signal-to-noise ratios can be countered if needed.

CONCLUSIONS

Phase mismatches sometimes occur between final processed sections and zero-phase synthetics based on well logs. This happens despite best efforts for controlled-phase acquisition and processing. The invoked controlled-phase strategies generally are based on deterministic corrections derived from field measurements and physical laws.

Kurtosis maximization by constant-phase rotation is a statistical method that can reveal the phase of a seismic wavelet. It is robust enough to detect time-varying phase changes. Phase-only corrections can then be applied by means of a time-varying phase rotation. Alternatively, amplitude and phase deconvolution can be achieved using time-varying Wiener filtering.

Naturally, a statistical analysis of the data alone cannot reveal whether a remnant phase indicates the data acquisition and processing strategy was unsuccessful or represents a true geologic feature. Nevertheless, a statistical approach yields relevant information about the data that can be used with zero-phase time-varying observations, as a quality control to check deterministic phase corrections, or even as an individual analysis tool. Time-varying wavelet extraction and deconvolution can also be a robust alternative to amplitude-only inverse-Q deconvolution. The latter tends to be unstable because it often attempts to restore information below the noise level of the data, e.g., amplitudes outside of the passband of the local wavelet. Time-varying wavelet extraction and deconvolution, on the other hand, only seeks to restore amplitudes within the local passband of the wavelet. It is therefore inherently stable.

ACKNOWLEDGMENTS

The author thanks the BG group, BP, Chevron, the Department of Trade and Industry, and Shell for financial support of the Blind Identification of Seismic Signals project. Discussions with Steve Campbell, Jeroen Goudswaard, and Dinh-Tuan Pham were very useful. Likewise, the comments and suggestions of Peter Cary, Mauricio Sacchi, and two anonymous reviewers helped to improve the original manuscript. The author is also grateful to Shell EP Europe for permission to use the data example.

REFERENCES

Arons, A. B., and D. R. Yennie, 1950, Phase distortion of acoustic pulses obliquely reflected from a medium with higher sound velocity: Journal of the Acoustical Society of America, **22**, 231–327.

Berkhout, A. J., 1977, Least-squares inverse filtering and wavelet deconvolution: Geophysics, **42**, 1369–1383.

Bickel, S. H., and R. R. Natarajan, 1985, Plane-wave Q deconvolution: Geophysics, **50**, 1426–1439.

Clarke, G. K. C., 1968, Time-varying deconvolution filters: Geophysics, **33**, 936–944.

Donoho, D., 1981, On minimum entropy deconvolution, *in* D. F. Findley, ed., Applied time series analysis II: Academic Press, 565–608.

Hargreaves, N. D., and A. J. Calvert, 1991, Inverse Q filtering by Fourier transform: Geophysics, **56**, 519–527.

Hauge, P., 1981, Measurements of attenuation from vertical seismic profiles: Geophysics, **46**, 1548–1558.

Levy, S., and D. W. Oldenburg, 1987, Automatic phase correction of common-midpoint stacked data: Geophysics, **52**, 51–59.

Longbottom, J., A. T. Walden, and R. E. White, 1988, Principles and application of maximum kurtosis phase estimation: Geophysical Prospecting, **36**, 115–138.

Quan, Y., and J. M. Harris, 1997, Seismic attenuation tomography using the frequency shift method: Geophysics, **62**, 895–905.

Robinson, J. C., 1979, A technique for the continuous representation of dispersion in seismic data: Geophysics, **44**, 1345–1351.

Sacchi, M. D., and T. J. Ulrych, 2000, Nonminimum-phase wavelet estimation using higher order statistics: The Leading Edge, **19**, 80–83.

Saggaf, M. M., and E. A. Robinson, 2000, A unified framework for the deconvolution of traces of nonwhite reflectivity: Geophysics, **65**, 1660–1676.

Tonn, R., 1991, The determination of the seismic quality factor Q from VSP data: A comparison of different computational methods: Geophysical Prospecting, **39**, 1–27.

Trantham, E. C., 1994, Controlled-phase acquisition and processing: 64th Annual International Meeting, SEG, Expanded Abstracts, 890–894.

Walden, A. T., and J. W. J. Hosken, 1985, An investigation of the spectral properties of primary reflection coefficients: Geophysical Prospecting, **33**, 400–435.

———, 1986, The nature of the non-Gaussianity of primary reflection coefficients and its significance for deconvolution: Geophysical Prospecting, **34**, 1038–1066.

Wang, R. J., 1969, The determination of optimum gate lengths for time-varying Wiener filtering: Geophysics, **34**, 683–695.

Wang, Y., 2002, A stable and efficient approach of inverse Q filtering: Geophysics, **67**, 657–663.

White, R. E., 1988, Maximum kurtosis phase correction: Geophysical Journal International, **95**, 371–389.

Wiggins, R., 1978, Minimum entropy deconvolution: Geoexploration, **16**, 21–35.

———, 1985, Entropy guided deconvolution: Geophysics, **50**, 2720–2726.